Heat Transfer in an Upper Convected Maxwell Fluid with Fluid Particle Suspension

K. Vajravelu[1,*], K. V. Prasad[2] and S. R. Santhi[3]

[1] *Department of Mathematics, Department of Mechanical, Materials and Aerospace Engineering, University of Central Florida, Orlando, FL 32816, USA*
[2] *Department of Mathematics, VSK University, Vinayaka Nagar, Bellary-583104, Karnataka, India*
[3] *Department of Mathematics, Bangalore University, Bangalore-560001, Karnataka, India*

Abstract. An analysis is carried out to study the magnetohydrodynamic (MHD) flow and heat transfer characteristics of an electrically conducting dusty non-Newtonian fluid, namely, the upper convected Maxwell (UCM) fluid over a stretching sheet. The stretching velocity and the temperature at the surface are assumed to vary linearly with the distance from the origin. Using a similarity transformation, the governing non-linear partial differential equations of the model problem are transformed into coupled non-linear ordinary differential equations and the equations are solved numerically by a second order finite difference implicit method known as the Keller-box method. Comparisons with the available results in the literature are presented as a special case. The effects of the physical parameters on the fluid velocity, the velocity of the dust particle, the density of the dust particle, the fluid temperature, the dust-phase temperature, the skin friction, and the wall-temperature gradient are presented through tables and graphs. It is observed that, Maxwell fluid reduces the wall-shear stress. Also, the fluid particle interaction reduces the fluid temperature in the boundary layer. Furthermore, the results obtained for the flow and heat transfer characteristics reveal many interesting behaviors that warrant further study on the non-Newtonian fluid flow phenomena, especially the dusty UCM fluid flow phenomena.

AMS subject classifications: 76W05, 76T20, 80A10

Key words: Heat transfer, hydromagnetic flow, UCM fluid, dusty fluid, fluid particle interaction.

*Corresponding author.
Email: kuppalapalle.vajravelu@ucf.edu (K. Vajravelu)

1 Introduction

The heat transfer due to a continuously moving surface through an ambient liquid is one of the important areas of current research due to its extensive application in broad spectrum of science and engineering disciplines, for instance, in chemical engineering processes like metallurgical process and polymer extrusion process involving cooling of a molten liquid being stretched into a cooling system. The fluid mechanical properties desired for an outcome of such a process would mainly depend on two aspects, one is the cooling liquid used and the other is the rate of stretching. Liquids of non-Newtonian characteristics, which are electrically conducting, can be opted as a cooling liquid as the flow and the heat transfer can be regulated by some external agency. Rate of stretching is very important as rapid stretching results in sudden solidification there by destroying the expected properties of the outcome. This is a fundamental problem that arises frequently in many practical situations such as polymer extrusion process; other processes like drawing; annealing and tinning of copper wires; continuous stretching; rolling and manufacturing of plastic films and artificial fibers; heat treated materials traveling on conveyer belts; glass blowing; crystal growing; paper production and so on. Sakiadis [1] was the first among the others to study the boundary layer flow generated by a continuous solid surface moving with constant velocity. Crane [2] extended the work of Sakiadis [1] and analyzed a steady two-dimensional boundary layer flow caused by a stretching sheet moving with a velocity linearly varying with the distance from a fixed point on the sheet. Many investigators have extended the work of Crane to study heat and mass transfer under different physical situations [3–7].

All the above investigators restricted their analyses to flow and heat transfer in the absence of magnetic field. But, we find several applications in polymer industry. To be more specific, it may be pointed out that many metallurgical processes involve the cooling of continuous strips or filaments by drawing them through a quiescent fluid and that in the process of drawing, these strips are sometimes stretched. Mention may be made of drawing, annealing, and thinning of copper wires. In these cases, the properties of final product depend to a great extent on the rate of cooling by drawing such strips in an electrically conducting fluid subject to a magnetic field. In view of these applications Pavlov [8] investigated the flow of an electrically conducting fluid caused solely by the stretching of an elastic sheet in the presence of a uniform magnetic field. Chakrabarti and Gupta [9] considered the flow and heat transfer of an electrically conducting fluid past a porous stretching sheet and presented analytical solution for the flow and numerical solution for the heat transfer problem. In this work the fluid was assumed to be Newtonian. However, many industrial fluids are non-Newtonian or rheological in nature: Such as molten plastics, polymers, suspension, foods, slurries, paints, glues, printing inks, blood. That is, they might exhibit dynamic deviation from Newtonian behavior depending upon the flow configuration and/or the rate of deformation. These fluids often obey non-linear constitutive equations and the complexity of these constitutive equations is the main culprit for the lack of exact analytical solutions. For example, visco-elastic

fluid models considered in these works are simple models, such as second order fluid model and Walters' model [10–13] which are known to be good for weakly elastic fluids subjected to slowly varying flows. These two models are known to violate certain rules of thermodynamics. Therefore significance of the results reported in the above works is limited as far as the polymer industry is concerned. Obviously for the theoretical results to be of any importance, more general visco-elastic fluid models such as upper convected Maxwell model or Oldroyd B model should be invoked in the analysis. Indeed these two fluid models are being used recently to study the visco-elastic fluid flow over a stretching or non-stretching sheet with or without heat transfer [14–20]. Recently, Prasad et al. [20] studied the effects of the temperature-dependent thermo-physical properties on the MHD boundary layer flow and heat transfer of a UCM fluid over a stretching sheet in the presence of internal heat generation/absorption.

All the above investigators restrict their analyses to the flow induced by a stretching sheet in the absence of fluid-particle suspension. The analysis of two-phase flow in which solid spherical particles are distributed in a fluid are of interest in a wide range of technical problems such as flow through packed beds, sedimentation, environmental pollution, centrifugal separation of particles and blood rheology. The study of the fluid-particle suspension flow is important in determining the particle accumulation and impingement of the particle on the surface. Saffman [21] investigated the stability of the laminar flow of a dusty gas in which the dust particles are uniformly distributed. Datta and Mishra [22] studied the dusty fluid flow over a semi-infinite flat plate. Vajravelu and Nayfeh [23] analyzed the hydromagnetic flow of dusty fluid over a stretching sheet with the effect of suction. Further Xie et al. [24] have extended the work of Datta and Mishra [22] to study the hydrodynamic stability of a particle-laden flow in growing flat plate boundary layer. Recently, Vajravelu et al. [25] studied the effects of variable viscosity and variable thermal conductivity on the hydromagnetic fluid-particle suspension flow and heat transfer over a stretching sheet. In these studies, the physical properties of the ambient fluid were assumed to be constant. However, it is known that these physical properties of the ambient fluid may change with temperature [26, 27]. For lubricating fluids, heat generated by internal friction and the corresponding rise in the temperature affects the thermal conductivity of the fluid so it can no longer be assumed constant. The increase of temperature leads to increase in the transport phenomena by reducing the thermal conductivity across the thermal boundary layer due to which the heat transfer at the wall is also affected. Therefore to predict the flow and heat transfer rates, it is necessary to take variable thermal conductivity of the fluid into account. Available literature on variable thermal conductivity and fluid-particle interaction shows that combined work has not been carried out for UCM fluid over a stretching sheet.

Motivated by these analyses, in the present paper, the authors study the MHD flow and heat transfer of a dusty non-Newtonian UCM fluid over a stretching sheet. This is in contrast to the work of Vajravelu and Nayfeh [22], where Newtonian fluid with constant thermal conductivity was considered. Because of the non-Newtonian rheology, the fluid-particle interaction, the momentum and energy equations for both the fluid and

the dust phase are coupled and highly non-linear partial differential equations (PDEs). These PDEs are converted to couple, non-linear ordinary differential equations (ODEs) by similarity variables. Because of the complexity and the non-linearly, we propose to solve these equations by a second order finite difference scheme known as the Keller-box method. The effects of pertinent parameters on the velocity and temperature fields, the skin friction coefficient and the local Nusselt number are presented in graphs and tables. It is believed that the results obtained in the present study will provide useful information for applications and will complement to the results in the literature.

2 Mathematical formulation

Consider a steady two-dimensional, boundary layer flow of a viscous incompressible and electrically conducting dusty non-Newtonian fluid (namely, UCM fluid) over a horizontal stretching sheet with a stretching velocity $U_w(x) = bx$, and prescribed surface temperature $T_w(x) = A(x/l)$, where $b > 0$ is the stretching velocity rate, l is the reference length scale, and A is a constant. The sheet is coinciding with the plane $y = 0$, with the flow being confined to $y > 0$. Two equal and opposite forces are introduced along the x-axis, so that the sheet is stretched, keeping the origin fixed (see Fig. 1). The thermo-physical fluid properties are assumed to be isotropic and constant, except for the thermal conductivity which is assumed to vary as a function of temperature in the following form (see [26])

$$K(T) = K_\infty \Big(1 + \frac{\varepsilon}{\Delta T}(T - T_\infty)\Big), \tag{2.1}$$

where $K(T)$ is the temperature dependent fluid thermal conductivity, K_∞ is the thermal conductivity far away from the slit, $\varepsilon = (K_w - K_\infty)/K_\infty$ is a small parameter known as the variable thermal conductivity parameter, K_w is the thermal conductivity at the surface, $\Delta T = T_w - T_\infty$, T_w is the surface temperature, and T_∞ is the ambient temperature. Further, the flow region is under the influence of a uniform transverse magnetic field $B = (0, B_0, 0)$: Imposition of such a magnetic field stabilizes the flow (see [16]). It is also assumed that
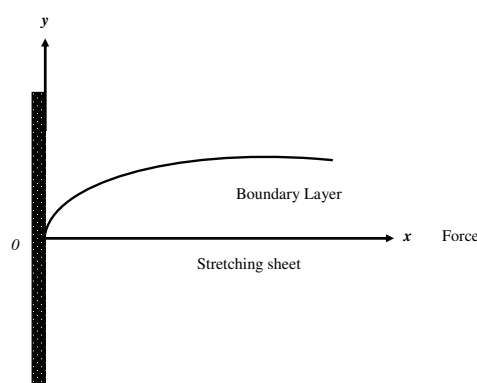

Figure 1: Physical model and co ordinate system.

the induced magnetic field is negligible: This is valid for small magnetic Reynolds number. Since there is no external electric field, the electric field due to polarization of charges is negligible. The viscous dissipation and the Ohmic heating terms are not included in the energy equation since they are, generally small. The fluid and the dust particle clouds are suppose to be static at the beginning. The dust particles are assumed to be spherical in shape and uniform in size and density of the dust particle is taken as a constant throughout the flow. Under these conditions, the basic boundary-layer equations for continuity, conservation of mass (with no pressure gradient), and energy for clear UCM fluid as well as dusty fluid can be written as

$$\frac{\partial u}{\partial x} + \frac{\partial v}{\partial y} = 0, \tag{2.2a}$$

$$u\frac{\partial u}{\partial x} + v\frac{\partial u}{\partial y} + \lambda\left(u^2\frac{\partial^2 u}{\partial x^2} + v^2\frac{\partial^2 u}{\partial y^2} + 2uv\frac{\partial^2 u}{\partial x\partial y}\right) = \nu\frac{\partial^2 u}{\partial y^2} - \frac{\sigma B_0^2}{\rho}\left(u + \lambda v\frac{\partial u}{\partial y}\right) - \frac{\rho_p}{\rho\tau}(u - u_p), \tag{2.2b}$$

$$u_p\frac{\partial u_p}{\partial x} + v_p\frac{\partial u_p}{\partial y} = \frac{1}{\tau}(u - u_p), \tag{2.2c}$$

$$u_p\frac{\partial v_p}{\partial x} + v_p\frac{\partial v_p}{\partial y} = \frac{1}{\tau}(v - v_p), \tag{2.2d}$$

$$\frac{\partial}{\partial x}(\rho_p u_p) + \frac{\partial}{\partial y}(\rho_p v_p) = 0, \tag{2.2e}$$

$$u\frac{\partial T}{\partial x} + v\frac{\partial T}{\partial y} = \frac{\partial}{\partial y}\left(\frac{K(T)}{\rho c_p}\frac{\partial T}{\partial y}\right) + \frac{\rho_p c_s}{\rho\gamma_T c_p}(T_P - T), \tag{2.2f}$$

$$u_p\frac{\partial T_p}{\partial x} + v_p\frac{\partial T_p}{\partial y} = -\frac{1}{\gamma_T}(T_P - T), \tag{2.2g}$$

where (u,v) and (u_p,v_p) are the velocity components of the fluid and dust particle phases along the x and y axes, respectively; and ρ is the density of the fluid. Here $\tau = 1/k$ is the relaxation time of particles, k is the Stokes' constant $(= 6\pi\mu D)$, μ is the coefficient of viscosity and D is the average radius of the dust particles. Further, σ is the electrical conductivity, λ is the relaxation time and ρ_p is the mass of the dust particles per unit volume of the fluid. T and T_p are respectively, the temperatures of the fluid and the dust phase particles. Further, c_p and c_s are, respectively, the specific heat capacity of the fluid and the specific heat capacity of the dust particles, γ_T is the temperature relaxation time $(= 3\mathrm{Pr}\gamma_p c_s/2c_p)$; γ_p is the velocity relaxation time $(= 1/k)$; and Pr is the usual Prandtl number. It may be pointed here that there is an additional term

$$\frac{\sigma B_0^2}{\rho}\lambda v\frac{\partial u}{\partial y}$$

in the momentum equation (2.2b) as in [16]. It is assumed that the normal stress is of the same order of magnitude as that of the shear stress. The last term in Eq. (2.2b) represents the force due to the relative motion between the fluid and the dust particles. In deriving these equations the Stokesian drag force is considered for the interaction between the fluid and the particle phases.

The appropriate boundary conditions on velocity and temperature are

$$u = U_w(x) = bx, \quad v = 0, \quad T = T_w = A(x/l), \qquad \text{at } y = 0, \qquad (2.3a)$$

$$u \to 0, \quad u_p \to 0, \quad v_p \to v, \quad \rho_p \to k\rho, \quad T \to T_\infty, \quad T_p \to T_\infty, \qquad \text{as } y \to \infty. \qquad (2.3b)$$

To convert the governing equations into a set of similarity equations, we introduce the following new variables

$$\eta = \sqrt{\frac{b}{\nu}} y, \qquad u = bx f'(\eta), \qquad v = -\sqrt{b\nu} f(\eta), \qquad (2.4a)$$

$$u_p = bx F(\eta), \qquad v_p = \sqrt{b\nu} G(\eta), \qquad \rho_r = H(\eta), \qquad (2.4b)$$

$$T - T_\infty = (T_w - T_\infty)\theta(\eta), \qquad T_P - T_\infty = (T_w - T_\infty)\theta_P(\eta), \qquad T_w - T_\infty = A(x/l), \qquad (2.4c)$$

where η is the similarity variable and prime denotes differentiation with respect to η, $\rho_r = \rho_p/\rho$ is the relative density, $f, F, G, H, \theta, \theta_p$ are dimensionless quantities and ν is the kinematic viscosity.

Substituting (2.4) into (2.2b)-(2.2g), we obtain the following coupled non-linear ordinary differential equation

$$f''' + ff'' - f'^2 + \beta_1(2ff'f'' - f^2 f''') - Mn(f' - \beta_1 ff'') + H\beta(F - f') = 0, \qquad (2.5a)$$

$$GF' + F^2 + \beta(F - f') = 0, \quad GG' + \beta(f + G) = 0, \quad GH' + HG' + FH = 0, \qquad (2.5b)$$

$$((1 + \varepsilon\theta)\theta')' - \Pr \begin{vmatrix} f' & \theta' \\ f & \theta \end{vmatrix} + \frac{2}{3}\beta H(\theta_P - \theta) = 0, \quad 2F\theta_P + G\theta_P' + L_0\beta(\theta_P - \theta) = 0, \qquad (2.5c)$$

along with the boundary conditions

$$f' = 1, \quad f = 0, \quad \theta = 1, \qquad \text{at } \eta = 0, \qquad (2.6a)$$

$$f' \to 0, \quad F \to 0, \quad G \to -f, \quad H \to k, \quad \theta \to 0, \quad \theta_P \to 0, \qquad \text{as } \eta \to \infty, \qquad (2.6b)$$

where $Mn = \sigma B_0^2/\rho b$ is the magnetic parameter, $\beta = 1/b\tau$ is the fluid-particle interaction parameter, $\beta_1 = \lambda b$ is the Maxwell parameter, $\Pr = \nu/\alpha_\infty$ is the Prandtl number and $L_0 = \tau/\gamma_T$ is the temperature relaxation parameter. The physical quantities of interest are the skin friction coefficient C_f and the local Nusselt number Nu_x which are defined by

$$C_f = \frac{\tau_w}{\rho_\infty U_w^2/2}, \quad Nu_x = \frac{xq_w}{k_\infty(T_w - T_\infty)}, \qquad (2.7)$$

where τ_w is the surface shear stress and q_w is the rate of heat transfer from the surface. The surface shear stress and the heat flux are given by

$$\tau_w = \mu_\infty \left(\frac{\partial u}{\partial y}\right)_{y=0}, \quad q_w = -K_\infty \left(\frac{\partial T}{\partial y}\right)_{y=0}. \qquad (2.8)$$

Using the similarity variables (2.4), we obtain

$$\frac{1}{2}C_f \text{Re}_x^{1/2} = f''(0) \quad \text{and} \quad \frac{Nu_x}{\text{Re}_x^{1/2}} = -\theta'(0), \qquad (2.9)$$

where $\text{Re}_x = U_w x/\nu$ is the local Reynolds number.

2.1 Exact solutions for some special cases

Here we present exact solutions in certain special cases. Such solutions are useful and serve as a baseline for comparison with the solutions obtained via numerical schemes.

2.1.1 No magnetic field and no fluid-particle interaction

In the limiting case of $\beta_1 = 0$ and $\beta = 0$, the MHD boundary layer flow and heat transfer problem degenerates. In this case the results of the present work are compared with the exact solution of Chakrabarti and Gupta [9] and are presented in Table 1. From this table it is obvious that the numerical solutions are in close agreement with the exact ones of [17, 19, 20] and [30].

Table 1: Comparison of some of the values of $-f''(0)$ when $\beta = 0.0$, $Pr = 1.0$ and $\varepsilon = 0.0$.

When $\beta_1 = 0.0$	$Mn = 0.0$	$Mn = 0.5$	$Mn = 1.0$	$Mn = 1.5$	$Mn = 2.0$
Andersson et al. [30] for $n = 1$	1.00000	1.2249	1.4140	1.58100	1.73200
Prasad et al. [20]	1.000174	1.224753	1.414499	1.581139	1.732203
Present results	1.000174	1.22475	1.41421	1.58114	1.73205
When $Mn = 0.0$	$\beta_1 = 0.0$	$\beta_1 = 0.2$	$\beta_1 = 0.4$	$\beta_1 = 0.6$	$\beta_1 = 0.8$
Sadeghy [17]	1.00000	1.0549	1.10084	1.0015016	1.19872
Vajravelu et al. [19]	1.0001743	1.051975	1.1019475	1.1501625	1.1967279
Present results	1.000174	1.05198	1.10195	1.15016	1.19673

2.1.2 No magnetic field but in the presence of fluid-particle interaction

In the absence of Maxwell parameter, the system in (2.5) reduces to those of Vajravelu et al. [25], when no variable thermo-physical properties are considered. Further, when the energy transfer and magnetic field are not considered, equations in (2.5) reduce to those of Vajravelu and Nayfeh [23]. Further, when the variable thermal conductivity and the Maxwell parameters are absent, the analytical solutions are obtained via perturbation technique for small values of fluid-particle interaction parameter. For small values of fluid-particle interaction parameter let us perturb the flow and heat transfer fields as

$$f = f_0 + \beta f_1 + 0(\beta^2), \qquad F = F_0 + \beta F_1 + 0(\beta^2), \qquad G = G_0 + \beta G_1 + 0(\beta^2), \qquad (2.10a)$$

$$H = H_0 + \beta H_1 + 0(\beta^2), \qquad \theta = \theta_0 + \beta \theta_1 + 0(\beta^2), \qquad \theta_p = \theta_{p0} + \beta \theta_{p1} + 0(\beta^2), \qquad (2.10b)$$

where the perturbations f_1, F_1, G_1 and H_1 are small compared with the mean or the zeroth-order quantities. With the help of equations in (2.10), the system of Eqs. (2.5) and the boundary conditions (2.6) become

$$f_0''' + f_0 f_0'' - (f_0')^2 - Mn f_0' = 0, \quad G_0 F_0' + F_0^2 = 0, \quad G_0 G_0' = 0, \qquad (2.11a)$$

$$G_0 H_0' + H_0 G_0' + F_0 H_0 = 0, \quad \theta_0'' + Pr(f_0 \theta_0' - f_0' \theta_0) = 0, \quad 2F_0 \theta_{p0} + G_0 \theta_{p0}' = 0, \qquad (2.11b)$$

$$f_0' = 1, \quad f_0 = 0, \quad \theta_0 = 1, \quad \text{at } \eta = 0, \qquad (2.11c)$$

$$f_0' \to 0, \quad F_0 \to 0, \quad G_0 \to -f_0, \quad H_0 \to k, \quad \theta_0 \to 0, \quad \theta_{p_0} \to 0, \quad \text{as } \eta \to \infty, \qquad (2.11d)$$

to the zeroth-order and

$$f_1''' + f_1 f_0'' + f_0 f_1'' - 2f_0' f_1' - Mn f_1' + H_0(F_0 - f_0') = 0, \tag{2.12a}$$

$$G_0 F_1' + G_1 F_0' + 2F_0 F_1 + F_0 - f_0' = 0, \tag{2.12b}$$

$$G_0 G_1' + G_0' G_1 + f_0 + G_0 = 0, \tag{2.12c}$$

$$G_0 H_1' + H_0' G_1 + H_0 G_1' + G_0' H_1 + F_0 H_1 + H_0 F_1 = 0, \tag{2.12d}$$

$$\theta_1'' + \Pr(f_0 \theta_1' - f_0' \theta_1) = \frac{2}{3} H_0(\theta_0 - \theta_{p0}) - \Pr(f_1 \theta_0' - f_1' \theta_0), \tag{2.12e}$$

$$G_0 \theta_{p1}' + F_0 \theta_{p1} = -F_1 \theta_{p0} - G_1 \theta_{p0}' + L_0(\theta_0 - \theta_{p0}), \tag{2.12f}$$

$$f_1' = 0, \quad f_1 = 0, \quad \theta_1 = 0, \quad \text{at } \eta = 0, \tag{2.12g}$$

$$f_1' \to 0, \quad F_1 \to 0, \quad G_1 \to -f_1, \quad H_1 \to k, \quad \theta_1 \to 0, \quad \theta_{p_1} \to 0, \quad \text{as } \eta \to \infty, \tag{2.12h}$$

to the first-order.

The exact solutions (in terms of Kummer's function ϕ) for the zeroth-order velocity components f_0, G_0, F_0, particle density H_0 and temperature θ_0 are

$$f_0 = A_1 + B_1 \exp(-\delta\eta), \quad F_0 = 0, \quad G_0 = -A_1, \quad H_0 = k, \tag{2.13a}$$

$$\theta_0 = \exp\left(-\frac{\Pr}{\delta}\eta\right) \frac{\phi\left(\frac{\Pr}{\delta^2} - 1, 1 + \frac{\Pr}{\delta^2}, -\frac{\Pr}{\delta^2} e^{-\delta\eta}\right)}{\phi\left(\frac{\Pr}{\delta^2} - 1, 1 + \frac{\Pr}{\delta^2}, -\frac{\Pr}{\delta^2}\right)}, \quad \theta_{p0} = 0, \tag{2.13b}$$

where $A_1 = 1/\delta$, $B_1 = -1/\delta$, $\delta = \sqrt{1 + Mn}$.

Similarly the exact solutions for the first-order velocity components, first-order particle density and first-order temperature, satisfying the differential equations and the boundary conditions are

$$f_1 = \left\{\frac{-kB_1}{(A_1\delta - B_1\delta + 2Mn)}\right\} e^{-\delta\eta} + \delta\eta e^{-\delta\eta} - 1, \quad F_1 = -\left(\frac{B_1}{A_1}\right) e^{-\delta\eta}, \tag{2.14a}$$

$$G_1 = -\left(\frac{B_1}{A_1}\right) e^{-\delta\eta} - \left\{\frac{-kB_1}{(A_1\delta - B_1\delta + 2Mn)}\right\}, \quad H_1 = 0, \quad \theta_{p1} = -\frac{L_0}{G_0} \int_\eta^\infty \theta_0(z)\,dz, \tag{2.14b}$$

where A_1, B_1, δ are constants. The solution θ_1 may be obtained by solving the inhomogeneous equation it satisfies, using the standard variation of parameter method. The results for various values of Mn, $\Pr$ and β_1 are compared with the available results in the literature, and are shown in Table 2. The results in Tables 1 and 2 reveal very good agreement between our numerical results and the available results in the literature.

3　Numerical procedure

The system (2.5) is coupled and highly nonlinear. Exact analytical solutions are not possible for the complete set of equations and, therefore, we use the efficient numerical method with second order finite difference scheme known as the Keller-box method [28, 29]. The

Table 2: Comparison of some of the values of $-\theta'(0)$ when $\beta=0.0$, $Mn=0.0$ and $\varepsilon=0.0$.

When $\beta_1=0.0$	Pr $=0.72$	Pr $=1.0$	Pr $=3.0$	Pr $=6.7$	Pr $=10.0$
Grubkha and Bobba [3]	0.8086	1.0000	1.9237	-	3.7207
Ali [6]	0.8058	0.9961	1.9144	-	3.7006
Ishak et al. [7]	0.8086	1.0000	1.9237	3.0003	3.7207
Present results	0.808836	1.000000	1.923687	3.000272	3.720788
When Pr $=1.0$	$\beta_1=0.0$	$\beta_1=0.2$	$\beta_1=0.4$	$\beta_1=0.6$	$\beta_1=0.8$
Vajravelu et al. [19]	1.0001743	0.9800923	0.9607879	0.9423181	0.9246983
Present results	1.000174	0.9800925	0.9607877	0.9423183	0.9246984

coupled non-linear ordinary differential equations (2.5) and (2.6) are reduced to a system of nine first order equations with nine unknowns by assuming $f=f_1$, $f'=f_2$, $f''=f_3$, $\theta=\theta_1$, $\theta'=\theta_2$. To solve this system of equations we require nine initial conditions while we have only two initial conditions $f(0)$, $f'(0)$ on f and one initial condition $\theta(0)$ on θ. The other six initial conditions $f''(0)$, $F(0)$, $G(0)$, $H(0)$, $\theta'(0)$ and $\theta_p(0)$ are not known. However, the values of $f'(\eta)$, $F(\eta)$, $G(\eta)$, $H(\eta)$, $\theta(\eta)$ and $\theta_p(\eta)$ are known as $\eta \to \infty$. We employ the Keller-box scheme and use the six known boundary conditions to produce six unknown initial conditions at $\eta=0$. To select η_∞, we begin with some initial guess values and solve the boundary value problem with some particular set of parameters to obtain $f''(0)$, $F(0)$, $G(0)$, $H(0)$, $\theta'(0)$ and $\theta_p(0)$. Thus, we start with the initial approximations as $f''(0)=\delta_1$, $F(0)=\delta_2$, $G(0)=\delta_3$, $H(0)=\delta_4$, $\theta'(0)=\delta_5$ and $\theta_p(0)=\delta_6$. Let δ_i ($i=1,2,3,4,5,6$) be the correct values of $f''(0)$, $F(0)$, $G(0)$, $H(0)$, $\theta'(0)$ and $\theta_p(0)$. We integrate the resulting system of nine ordinary differential equations using the fourth-order Runge-Kutta method and obtain the values of $f''(0)$, $F(0)$, $G(0)$, $H(0)$, $\theta'(0)$ and $\theta_p(0)$. The solution process is repeated with another larger value of η_∞ until two successive values of $f''(0)$, $F(0)$, $G(0)$, $H(0)$, $\theta'(0)$ and $\theta_p(0)$ differ only after desired digit signifying the limit of the boundary along η. The last value of η_∞ is chosen as the appropriate value for that particular set of parameters. Finally, the problem can be solved numerically using a second-order finite difference scheme known as the Keller-box method. The numerical solutions are obtained in four steps as follows:

- Reduce the system (2.5) to a system of first order equations.
- Write the difference equations using central differences.
- Linearize the algebraic equations by Newton's method, and write them in matrix-vector form.
- Solve the linear system by the block tri-diagonal elimination technique.

For the sake of brevity, the details of the numerical procedure are not presented here. It is also important to note that the computational time for each set of input parameters should be short. Because physical domain in this problem is unbounded, whereas the computational domain has to be finite, we apply the far field boundary conditions for the similarity variable η at finite value denoted by $\eta_{\max}$. We ran our bulk of computations

with the value $\eta_{\max} = 7$, which is sufficient to achieve the far field boundary conditions asymptotically for all values of the parameters considered. For numerical calculations, a uniform step size of $\Delta\eta = 0.01$ is found to be satisfactory and the solutions are obtained with an error tolerance of 10^{-6} in all the cases. The accuracy of the numerical scheme is validated by comparing the skin friction and the rate of heat transfer results with those available in the literature: They agree very well (see Tables 1 and 2).

4   Discussion of the results

In this section, we illustrate the effects of the pertinent parameters, namely, the fluid-particle interaction parameter β, the Maxwell parameter β_1, the magnetic parameter Mn, the variable thermal conductivity parameter ε, and the Prandtl number Pr on the flow

Table 3: Numerical values for skin friction $f''(0)$, the particle velocity components $F(0)$, $G(0)$, the particle density component $H(0)$, the wall temperature gradient $\theta(0)$, and the wall temperature dust particles $\theta_p(0)$ for different values of the physical parameters.

| Pr	ε	β_l	Mn	β	$f''(0)$	$F(0)$	$G(0)$	$H(0)$	$\theta'(0)$	$\theta_p(0)$
				0.0	-1.05198	0.00000	-0.91721	0.20000	-0.91331	0.00000
			0.0	0.2	-1.06772	0.16766	-0.74287	0.20335	-0.97889	0.12794
1.0	0.1	0.2		1.0	-1.10203	0.52204	-0.30747	0.26545	-1.11558	0.41699
				0.0	-1.47454	0.00000	-0.65650	0.20000	0.80837	0.00000
			1.0	0.2	-1.48586	0.16766	-0.53473	0.20335	-0.88773	0.18858
				1.0	-1.51082	0.52207	-0.22422	0.26538	-1.02239	0.47543
				0.0	-1.22475	0.00000	-0.81593	0.20000	-0.87683	0.00000
		0.0	0.5	0.2	-1.23838	0.16746	-0.66061	0.20341	-0.94702	0.1469
1.0	0.1			1.0	-1.26830	0.52143	-0.27293	0.26617	-1.08360	0.43885
				0.0	-1.48979	0.00000	-0.59761	0.20000	-0.77975	0.00000
		1.0	0.5	0.2	-1.50079	0.16813	-049030	0.20319	-0.86330	0.20926
				1.0	-1.52507	0.52368	-0.20987	0.26349	-0.99637	0.48877
				0.0	-1.28083	0.00000	-0.75394	0.20000	-0.92319	0.00000
	0.0	0.2	0.5	0.2	-1.29379	0.16766	-0.61381	0.20335	-0.99709	0.15460
1.0				1.0	-1.32237	0.52207	-0.25617	0.26537	-1.14308	0.44341
				0.0	-1.28083	0.00000	-0.75394	0.20000	-0.71619	0.00000
	0.4	0.2	0.5	0.2	-1.29379	0.16766	-0.61381	0.20335	-0.77751	0.71511
				1.0	-1.32237	0.52207	-0.25617	0.26537	-0.89403	0.46915
				0.0	-1.22475	0.00000	-0.81593	0.20000	-0.70200	0.00000
0.72	0.1	0.2	0.2	0.2	-1.29379	0.16766	-0.61381	0.20335	-0.76722	0.24194
				1.0	-1.28833	0.70817	-0.06469	0.52063	-0.90682	0.54564
				0.0	-1.22475	0.00000	-0.81593	0.20000	-2.33917	0.00000
5.0	0.1	0.2	0.2	0.2	-1.29379	0.16766	-0.61381	0.20335	-2.34460	0.01386
				1.0	-1.28833	0.70817	-0.06469	0.52063	-2.45253	0.08022
				0.0	-1.22475	0.00000	-0.81593	0.20000	-3.43155	0.00000
10.0	0.1	0.2	0.2	0.2	-1.29379	0.16766	-0.61381	0.20335	-3.42930	0.00473
				1.0	-1.28833	0.70817	-0.06469	0.52063	-3.50713	0.03229
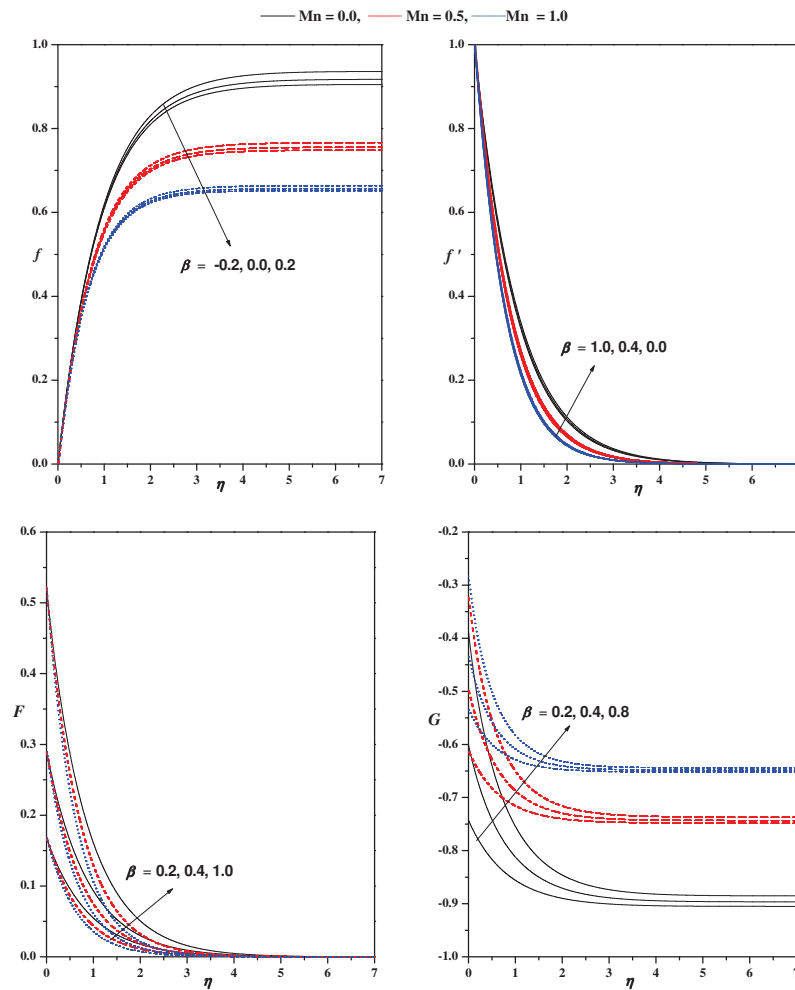
Figure 2: From left to right: (a) Transverse velocity profiles for different values of β and Mn when $\beta_1 = 0.2$, $\Pr = 1.0$, $\varepsilon = 0.1$; (b) Horizontal velocity profiles for different values of β and Mn when $\beta_1 = 0.2$, $\Pr = 1.0$, $\varepsilon = 0.1$; (c) Particle velocity components F for different values of β and Mn when $\beta_1 = 0.2$, $\Pr = 1.0$, $\varepsilon = 0.1$; (d) Particle velocity components G for different values of β and Mn when $\beta = 0.2$, $\Pr = 1.0$, $\varepsilon = 0.1$.

and heat transfer of the UCM fluid over a horizontal stretching sheet. The temperature relaxation parameter L_0 is chosen to be unity throughout the computation. In order to analyze the salient features of the problem, the numerical results are illustrated graphically in Figs. 2-6. Also the numerical results for the skin friction, the particle velocity and the density components, the fluid temperature, and the dust-phase temperature at the surface for different values of the physical parameters are recorded in Table 3.

The transverse velocity $f(\eta)$, the horizontal velocity $f'(\eta)$, the particle transverse velocity $F(\eta)$ and the particle horizontal velocity $G(\eta)$ profiles are shown in Figs. 2(a)-(d) for different values of Mn and β. The general trend is that $f'(\eta)$, $F(\eta)$ and $G(\eta)$ decrease
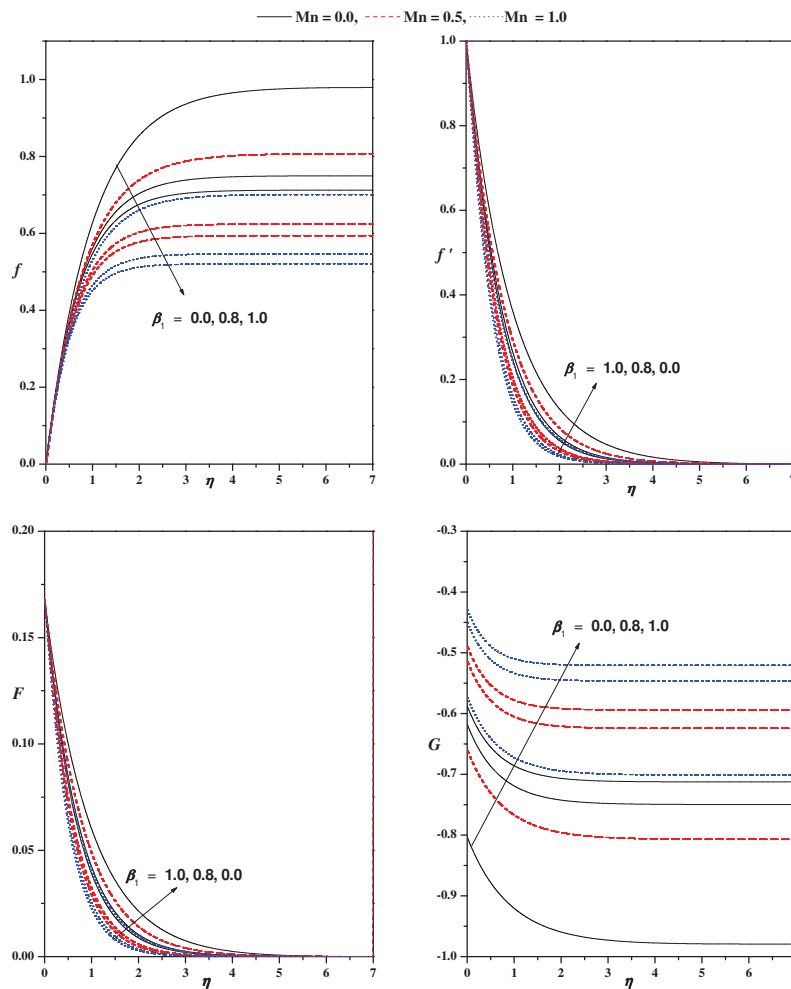
Figure 3: From left to right: (a) Transverse velocity profiles for different values of β_1 and Mn when $\beta=0.2$, $Pr=1.0$, $\varepsilon=0.1$; (b) Horizontal velocity profiles for different values of β_1 and Mn when $\beta=0.2$, $Pr=1.0$, $\varepsilon=0.1$; (c) Particle velocity components F for different values of β_1 and Mn when $\beta=0.2$, $Pr=1.0$, $\varepsilon=0.1$; (d) Particle velocity components G for different values of β_1 and Mn when $\beta=0.2$, $Pr=1.0$, $\varepsilon=0.1$.

monotonically as the distance increases from the surface, whereas $f(\eta)$ increases as the distance increases from stretching sheet. It is observed from these figures that $f'(\eta)$ and $F(\eta)$ profiles decrease with an increase in Mn. This observation holds true even with particle velocity component $F(\eta)$; but quite the opposite is true with $G(\eta)$. Physically it means that the induction of transverse magnetic field (normal to the flow direction) has a tendency to induce a drag, known as the Lorentz force, which tends to resist the flow. It is noticed that the effect of increasing values of β is to reduce the thickness of the fluid velocity in the boundary layer and increase the dust-phase transverse velocity, as well as the horizontal velocity component.
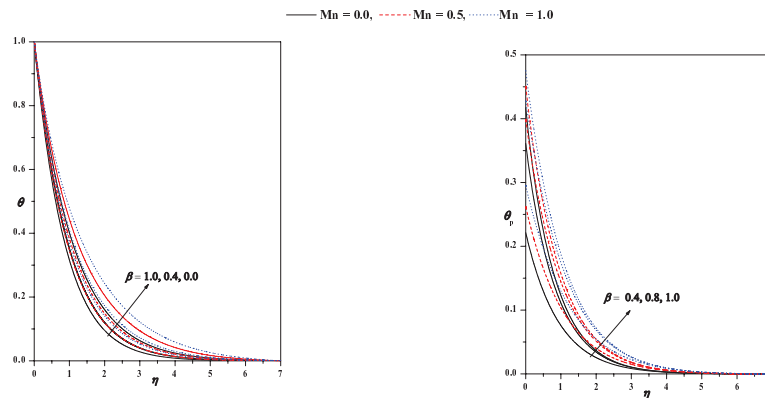
Figure 4: From left to right: (a) Fluid temperature profiles for different values of β and Mn when $\beta_1 = 0.2$, $\Pr = 1.0$, $\varepsilon = 0.1$; (b) Dust-phase temperature profiles for different values of β and Mn when $\beta_1 = 0.2$, $\Pr = 1.0$, $\varepsilon = 0.1$.
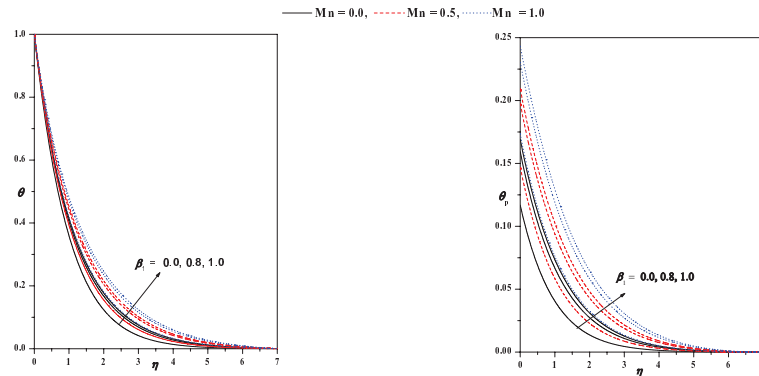

Figure 5: From left to right: (a) Fluid temperature profiles for different values of β_1 and Mn when $\beta = 0.2$, $\Pr = 1.0$, $\varepsilon = 0.1$; (b) Dust-phase temperature profiles for different values of β_1 and Mn when $\beta = 0.2$, $\Pr = 1.0$, $\varepsilon = 0.1$.

Figs. 3(a)-(d) exhibit the transverse velocity $f(\eta)$, the horizontal velocity $f'(\eta)$, the particle transverse velocity $F(\eta)$ and the particle horizontal velocity $G(\eta)$ profiles for several sets of values of Mn and β_1. The effect of the magnetic field on the velocity of the fluid elements above the sheet appears to become less pronounced for the Maxwell fluid, i.e., by an increase in the elasticity level of the fluid. That is to say that larger velocity can be expected to arise in MHD flows over stretching sheets if the fluid is elastic. It is evident from the Figs. 3(a)-(d) that the effect of increasing values of the Maxwell parameter is to reduce the fluid velocity in the boundary layer and the dust-phase horizontal velocity, but quite opposite is found in dust-phase transverse velocity.

Figs. 4-6 show the fluid temperature $\theta(\eta)$ and dust-phase temperature $\theta_p(\eta)$ profiles for different values of the governing parameters. The general trend is that the fluid-temperature distribution is unity at the surface, whereas the dust-phase temperature is
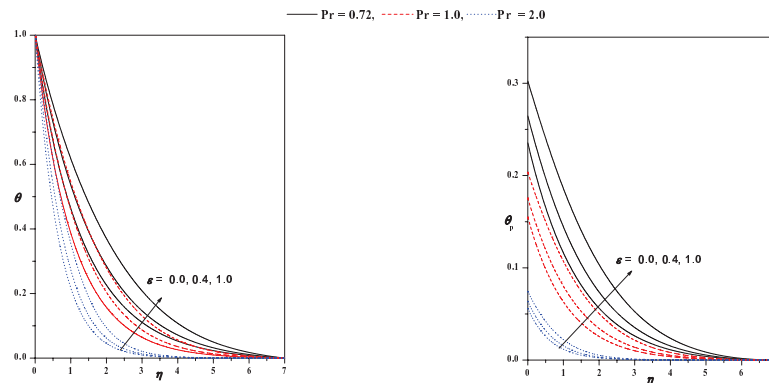
Figure 6: From left to right: (a) Fluid temperature profiles for different values of ε and Pr when $\beta = 0.2$, $Mn = 1.0$, $\beta_1 = 0.2$; (b) Dust-phase temperature profiles for different values of ε and Pr when $\beta = 0.2$, $Mn = 0.5$, $\beta_1 = 0.2$.

not. However, with the changes in the governing parameters both asymptotically tend to zero as the distance increases from the boundary. Figs. 4(a) and (b) illustrate the effect of Mn and β on $\theta(\eta)$. The effect of increasing values of Mn is to increase $\theta(\eta)$ and also $\theta_p(\eta)$. From the graphical representation, the magnetic field has a significant effect on the temperature field. As explained above, the transverse magnetic field gives rise to a resistive force known as the Lorentz force. This force makes the fluid experience a resistance by increasing the friction between its layers. Hence, there is an increase in the temperature profile as well as the dust-phase profile. The effect of β is to decrease the temperature profile that in turn reduces the thickness of the thermal boundary, whereas it enhances the dust-phase temperature at the surface: Thus increases the thickness of the dust-phase temperature.

Figs. 5(a) and (b) exhibit the fluid-temperature distribution and the dust-phase temperature distribution for several sets of values of the Mn and β_1. The effect of the magnetic field on the temperature field is less significant for Maxwell fluid, i.e., for elastic liquids. The effect of β_1 is to increase the fluid temperature and the dust-phase temperature. This is due to the fact that the thickening of the thermal boundary layer occurs due to an increase in the elasticity stress parameter. However, the temperature distribution asymptotically tends to zero as the distance increases from the boundary. The graphs for $\theta(\eta)$ and $\theta_p(\eta)$ for different values of ε and Pr are shown in Figs. 6(a) and (b). These figures demonstrate that an increase in ε results in an increase in the temperature $\theta(\eta)$ as well as in $\theta_p(\eta)$. This is due to the fact that the assumption of temperature dependent thermal conductivity implies a reduction in the magnitude of the transverse velocity by a quantity $\partial K(T)/\partial y$ as can be seen from the energy equation. Also, we observe that the effect of Pr is to decrease both $\theta(\eta)$ and $\theta_p(\eta)$. Finally, the effects of all the physical parameters on the surface-velocity gradient, the particle-velocity components, particle-density component, the temperature gradient, and the dust-phase temperature at the sheet are

presented in Table 3. It is of interest to note that the effect β_1, Mn and β is to increase the magnitude of the skin friction coefficient. However, the effect of ε, β_1 and Mn is to decrease the magnitude of the temperature gradient at the sheet; but the reverse trend is observed with an increase in Pr and β. From Table 3, it is further noticed that the effect of Mn and β is to increase the dust-phase temperature and the particle velocity component.

5   Conclusions

Some of the interesting observations are:

- The effect of the fluid-particle interaction and the magnetic field in the Maxwell fluid flow is to decrease the fluid velocity in the boundary layer.
- The fluid-particle interaction reduces the fluid temperature: But, quite opposite is true in particle phase temperature.
- The variable thermal conductivity enhances the fluid temperature and the particle phase temperature in the flow region.
- The thermal boundary layers of the fluid and the dust phase are significantly affected by the Prandtl number and its effect is to decrease the thermal boundary layer thickness.

Nomenclature

A, A_1, B_1	constants
B_0	uniform magnetic field
b	stretching rate, positive constant
C_f	skin-friction
c_p	specific heat capacity of the fluid
c_s	specific heat capacity of the dust particles
D	average radius of the dust particles
f	dimensionless stream function
F, G	particle velocity component
H	particle density components
k	Stokes' resistance
$K(T)$	thermal conductivity
K_∞	thermal conductivity of the fluid far away from the sheet
k_w	thermal conductivity at the surface

l	reference length scale
L_0	temperature relaxation parameter
Mn	magnetic parameter
Nu_x	Nusselt number
Pr	Prandtl number
q_w	heat transfer from the surface of the sheet
Re_x	local Reynolds number
T	fluid temperature
T_p	temperature of the dust particle
$T_w(x)$	temperature of the stretching sheet
T_∞	ambient temperature
u, v	velocity components in the x, y direction
u_p, v_p	velocity components of the dust particles in the x, y direction
$U_w(x)$	velocity of the stretching sheet
x, y	cartesian coordinates
$\alpha(T)$	temperature dependent thermal diffusivity
β	fluid particle interaction parameter
β_1	Maxwell parameter
γ_p	velocity relaxation time
γ_T	temperature relaxation time
$\delta_i \ (i=1 \text{ to } 6)$	unknown initial conditions
δ	constant defined in Eq. (2.10)
ν_∞	kinematic viscosity
ρ_p	density of the particle phase
ρ_r	relative density
ρ_∞	density of the fluid
σ	electric conductivity
η	similarity variable
λ	relaxation time of fluid
ΔT	characteristic temperature
ε	variable thermal conductivity parameter
θ	dimensionless fluid temperature
θ_p	dimensionless dust-phase temperature
ϕ	confluent hypergeometric function
μ_∞	coefficient of viscosity

τ	relaxation time of particles
τ_w	skin friction or shear stress
w	condition at the stretching surface
∞	condition at infinity
$'$	differentiation with respect to η

Acknowledgements

References

[1] B. C. SAKIADIS, *Boundary-layer behavior on continuous solid surfaces I, The boundary layer on a equations for two dimensional and axisymmetric flow*, AIChE. J., 7 (1961), pp. 26–28.

[2] L. J. CRANE, *Flow past a stretching plate,* ZAMP, 1 (1970), pp. 645–647.

[3] L. G. GRUBKA AND K. M. BOBBA, *Heat transfer characteristics of a continuous stretching surface with variable temperature*, ASME J. Heat Trans., 107 (1985), pp. 248–250.

[4] B. K. DUTTA, P. ROY AND A. S. GUPTA, *Temperature field in flow over a stretching sheet with uniform heat flux,* Int. Comm. Heat Mass Trans., 12 (1985), pp. 89–94.

[5] C. K. CHEN AND M. I. CHAR, *Heat transfer of a continuous stretching surface with suction or blowing,* J. Math. Anal. Appl., 135 (1988), pp. 568–580.

[6] M. E. ALI, *Heat transfer characteristics of a continuous stretching surface,* Heat Mass Trans., 29 (1994), pp. 227–234.

[7] A. ISHAK, R. NAZAR AND I. POP, *Boundary layer flow and heat transfer over an unsteady stretching vertical surface,* Meccanica, 44 (2009), pp. 369–375.

[8] K. B. PAVLOV, *Magnetohydrodynamic flow of an incompressible viscous fluid caused by deformation of a plane surface,* Magnitnaya Gidrodinamika (USSR), 4 (1974), pp. 146–147.

[9] A. CHAKRABARTI AND A. S. GUPTA, *Hydromagnetic flow and heat transfer over a stretching sheet,* Quart. Appl. Math., 37 (1979), pp. 73–78.

[10] K. R. RAJAGOPAL, T. Y. NA AND A. S. GUPTA, *Flow of a visco-elastic fluid over a stretching sheet*, Rheol. Acta, 23 (1984), pp. 213–215.

[11] B. S. DANDAPAT AND A. S. GUPTA, *Flow and heat transfer in a visco-elastic fluid over a stretching sheet,* Int. J. Non-Linear Mech., 24 (1989), pp. 215–219.

[12] M. I. CHAR, *Heat and mass transfer in a hydromagnetic flow of a visco-elastic fluid over a stretching sheet*, J. Math. Anal. Appl., 186 (1994), pp. 674–689.

[13] R. CORTELL, *A note on magnetohydrodynamic flow of a power law fluid over a stretching sheet*, Appl. Math. Comput., 168 (2005), pp. 557–566.

[14] R. K. BHATNAGAR, G. GUPT AND K. R. RAJAGOPAL, *Flow of an Oldroyd-B fluid due to a stretching sheet in the presence of a free stream velocity,* Int. J. Non-Linear Mech., 30 (1995), pp. 391–405.

[15] M. RENARDY, *High weissenberg number boundary layers for upper convected Maxwell fluid,* J. Non-Newtonian Mech., 68 (1997), pp. 125–132.

[16] T. Hayat, Z. Abbas and M. Sajid, *Series solution for the upper-convected Maxwell fluid over a porous stretching plate,* Phys. Lett. A, 358 (2006), pp. 396–403.

[17] K. Sadeghy, A. H. Najafi and M. Saffaripour, *Sakiadis flow of an upper-convected Maxwell fluid*, Int. J. Non-Linear Mech., 40 (2005), pp. 1220–1228

[18] V. Aliakbar, A. Alizadeh-Pahlavan and K. Sadeghy, *The influence of thermal radiation on MHD flow of Maxwellian fluids above stretching sheets,* Comm. Non-linear Sci. Numer. Simulation, 14 (2009), pp. 779–794.

[19] K. Vajravelu, K. V. Prasad and A. Sujatha, *Convection heat transfer in a Maxwell fluid at a non-isothermal surface,* Cent. Euro. J. Phys., 9 (2011), pp. 807–815.

[20] K. V. Prasad, A. Sujatha, K. Vajravelu and I. Pop, *MHD flow and heat transfer of a UCM fluid over a stretching surface with variable thermophysical properties,* Meccanica, 47 (2012), pp. 1425–1439.

[21] P. G. Saffman, *On the stability of laminar flow of a dusty gas*, J. Fluid. Mech., 13 (1962), pp. 120–128.

[22] N. Datta and S. K. Mishra, *Boundary layer flow of a dusty fluid over a semi-infinite flat plate,* Acta Mech., 42 (1982), pp. 71–83.

[23] K. Vajravelu and J. Nayfeh, *Hydromagnetic flow of a dusty fluid over a stretching sheet,* Int. J. Non-Linear Mech., 27 (1992), pp. 937–945.

[24] Xie Ming-Liang, Lin Jian-Zhong and Xing Fu-Tang, *On the hydrodynamic stability of a particle-laden flow in growing flat plate boundary layer,* J. Zhejiang Uni. SCI. A, 8 (2007), pp. 275–284.

[25] K. Vajravelu, K. V. Prasad and P. S. Datti, *Hydromagnetic fluid flow and heat transfer at a stretching sheet with fluid-particle suspension and variable fluid properties*, J. Fluids Eng., 134 (2012), pp. 121001–121003.

[26] T. C. Chiam, *Heat transfer in a fluid with variable thermal conductivity over a stretching sheet,* Acta Mech., 29 (1998), pp. 63–72.

[27] K. Vajravelu, K. V. Prasad and S. R. Santhi, *Axisymmetric magneto-hydrodynamic (MHD) flow and heat transfer at a non-isothermal stretching cylinder,* Appl. Math. Comput., 219 (2012), pp. 3993–4005.

[28] T. Cebeci and P. Bradshaw, Physical and Computational Aspects of Convective Heat Transfer, Springer-Verlag, New York, 1984.

[29] H. B. Keller, Numerical Methods for Two-Point Boundary Value Problems, Dover Publ., New York, 1992.

[30] H. I. Andersson, K. H. Bech and B. S. Dandapat, *Magneto-hydrodynamic flow of a power law fluid over a stretching sheet,* Int. J. Non-Linear Mech., 27 (1992), pp. 929–936.